J Mater Sci (2009) 44:6512–6518
DOI 10.1007/s10853-009-3596-3

MESOSTRUCTURED MATERIALS

Direct synthesis of Cr-MCM-48-like large pore mesoporous silica

Lingzhi Wang · Lei Wang · Jinlong Zhang

Received: 28 November 2008 / Accepted: 14 May 2009 / Published online: 2 June 2009

Abstract Chromium-substituted MCM-48-like large pore mesoporous silica with average pore size up to 10 nm was directly synthesized by using P123 ($EO_{20}PO_{70}EO_{20}$) as a template, *n*-butanol as an assistant, and chromic nitrate nonahydrate as a chromium source. The Cr species was doped by simply adjusting the pH of the synthesis system with ammonia from strong acid to nearly neutral after crystallization for 24 h. The Si/Cr ratios in the initial gel ranged from 10 to 80, and the actual weight percentage of Cr was analyzed by ICP. XRD pattern, high-resolution TEM, and N_2 adsorption–desorption isotherm were employed to investigate the pore structure properties of these materials. The results showed that all the samples had *Ia3d* cubic structure and the pore channels were highly ordered. UV–vis, wide-angle XRD, and ESR spectra revealed that at lower Cr content (Si/Cr $>$ 30), only Cr (VI) and Cr(V) species existed in the mesoporous framework, and at higher Cr content, Cr (III) species appeared.

Introduction

The emergence of porous silica materials with 2–50-nm-ordered pore structure meets the increasing demands of applications involving large molecules in various fields. The milestones of the development of these types of materials were the invention of M41S in 1992 and SBA-15 in 1998 [1, 2], which were synthesized in strong basic and acidic conditions, respectively. These materials were widely studied on their preparations, structures, and applications. Among them, MCM-41 and SBA-15 have similar hexagonal *P6 mm* symmetry pore structure; however, MCM-41 seems inferior to SBA-15 in catalysis applications concerned with aqueous system due to its comparatively small pore size (<5 nm) and thin pore walls (<2 nm). The flourishing development of the SBA-15 mainly benefits from its wide pore size range from 5 to 30 nm and thick walls, making it more robust and applicable. On the other hand, to solve the problem of pore blockage of SBA-15 caused by the one-dimensional straight pore channel, three-dimensional interwoven mesoporous structure with *Ia3d* symmetry was also synthesized in the conditions similar to SBA-15. These materials have the same pore structure with MCM-48, one of the M41S type, but have larger pore and thicker walls similar to SBA-15. Besides the structure-directing agent, P123, the preparation of the above MCM-48-like large pore materials needs some additives such as organosiloxane, NaI salt, *n*-butanol or anionic sodium dodecyl sulfate (SDS) [3–6]; otherwise, no *Ia3d* mesostructure forms. The action of these additives is to transform the hexagonal phase to cubic phase by improving the hydrophobicity of P123. Moreover, it was reported that using a self-made diblock copolymer can also lead to the formation of MCM-48-like large pore materials without additives [7].

On the other hand, pure silica materials are usually catalytically inert, but can be endowed with catalytic activity by incorporating transition-metal atom into the framework. These metal-doped mesoporous materials have great application perspective in macromolecular catalysis, especially for the above MCM-48-like material with highly interwoven pore structure and large pore size. At present, direct synthesis and post-synthesis are the two alternative methods for the introduction of heteroatom into the

L. Wang · L. Wang · J. Zhang (✉)
Lab for Advanced Materials and Institute of Fine Chemicals, East China University of Science and Technology, 130 Meilong Road, Shanghai 200237, People's Republic of China
e-mail: jlzhang@ecust.edu.cn

mesoporous material. It is obvious that direct synthesis is a more convenient method. However, for the material obtained from acid system, direct synthesis method is difficult because the metal oxides tend to decompose into metal ions and cannot be effectively incorporated into mesoporous material. Inspite of this difficulty, some efforts have been made to directly synthesize heteroatom-doped mesoporous silica materials in acid system. For example, Yue et al. [8] obtained aluminum-doped SBA-15 through direct synthesis for the first time at pH 1.5. Xiao et al. [9] used a complex method to synthesize Al-substituted SBA-15-like materials in which the framework consisted of nanocrystalline ZSM-5. Newalkar et al. [10] have recently obtained Ti-containing SBA-15 materials using a microwave-assisted synthetic method. Li et al. [11] used fluoride as the additive for the direct synthesis of Ti-substituted SBA-15, but it is still need to be carried out in strong acid conditions. Xiao et al. [12] directly synthesized Al-substituted SBA-15 by a pH-adjusting method using ammonia as the pH-adjusting agent. Moreover, in consideration of the strict synthesis conditions of metal-doped mesoporous material in acidic system, various post-synthesis grafting procedures have also been performed for mesoporous materials. For example, by using wet impregnation method in water or ethanol solutions, various metals such as V [13], Ce [14], Cr [15], and Co [16] were incorporated into the mesoporous materials. Zhu et al. [17, 18] reported that a large amount of metal could be incorporated into the framework of mesoporous materials by using solid-state inclusion method. Moreover, metal oxide nanoparticles or nanowires were also loaded into the mesoporous channel by using post-synthesis procedures [19, 20]. Although the metal can be substantially loaded onto the matrix, most of the post-treatment methods are troublesome and the ordering of the sample may be seriously destroyed.

Compared with one-dimensional mesostructure such as SBA-15, the interwoven channel structure of *Ia3d* cubic symmetry material is more attractive in the field of catalysis, especially for that has larger pore and thicker walls. However, direct synthesis of metal-doped MCM-48-like large pore materials is challenging. Recently, Zhu et al. [21] directly prepared metal-oxide loading large pore MCM-48 by adding acetate salt to the synthesis system similar to SBA-15. Acetate salt not only triggered the phase transformation from hexagonal p6 mm to cubic *Ia3d*, but also played the roles of metal precursor and system pH-tuning agent. In that system, great amount of acetate should be added to assure the formation of cubic phase and increase the system pH to form metal oxide in the pore channel. However, high concentration of acetate salt is more easily to form large-size metal oxide, which leads to the pore blockage and is disadvantageous for the catalysis effect. Here, we report the synthesis of single site and low poly chromium oxide–silica heterogeneous catalysis based on MCM-48-like large pore material in the acid system by using P123 as a template, *n*-butanol as an assistant for the formation of cubic phase, chromic nitrate as a chromium source, and ammonia as the pH-adjusting agent for the deposition of Cr species in the mesoporous channel. We selected Cr by considering its good performance as a redox catalyst, which is widely used in many catalytic reactions such as dehydrogenation of propane to form propylene and oxidation of cyclohexane to form cyclohexanol [22, 23]. Up to now, this is the first report for the formation of metal-doped MCM-48-like large pore mesoporous material by pH-adjusting method with ammonium, and our result shows that this method is simple and effective for the formation of single site and low poly chromium oxide–silica heterogeneous catalysis instead of only large-size chromium oxide in the acid system.

Experimental

Chromium-incorporated mesoporous silica was synthesized using 1.5 g of triblock copolymer P123 as template, which was dissolved into 60 mL of 1 M HCl. The mixture was stirred at 35 °C into a clear solution, and then a certain amount of *n*-butanol was added. After stirring for 1 h, 3.3-mL tetraethyl orthosilicate (TEOS) was mixed with the solution just after the addition of required amount of solid $Cr(NO_3)_3{\cdot}9H_2O$. The mixture was stirred at 35 °C for 1 day. The molar composition of the final gel mixture was 1.0TEOS:0.017P123:0.013–0.10Cr:4.05HCl:1.0*n*-BuOH:217H_2O. The mixture was then transferred into an autoclave for further condensation at 100 °C for 1 day. After the procedure described above, the pH of the system was adjusted up to the required value by adding 7 wt% ammonia dropwise at room temperature, and the obtained mixture was hydrothermally treated again at 100 °C for one more day. The final solid was collected by filtration, washed with water, and dried at 100 °C for 24 h. The surfactants were removed by calcination at 550 °C in air for 5 h.

Powder X-ray diffraction (XRD) patterns of all the samples were recorded on Rigaku D/MAX-2550 diffractometer using Cu Ka radiation of wavelength 0.1541 nm, typically, running at a voltage of 40 kV and current of 100 mA. N_2 adsorption and desorption isotherms were carried out using TriStar 3000 system by N_2 physisorption at 77 K. For BET (Brunauer–Emmett–Teller method) test, the calcined samples were outgassed to remove moistures and impurities at 473 K for 5 h before measurement. The diffuse reflectance UV–vis spectroscopy was recorded with Varian Cary 500. The ESR spectra were obtained from an equipment of Bruker BioSpin GmbH. Transmission

electron micrographs (TEM) were taken on a 2000 JEOL electron microscope operating at 200 kV. The samples for TEM were prepared by dispersing a large number of particles in alcohol, and depositing onto a holey carbon film on a Cu grid.

Results and discussion

Figure 1 shows XRD patterns of the calcined samples synthesized with different Si/Cr molar ratios by adjusting the pH value to 6. It can be observed that all the samples show clear (211) and (220) peaks, which indicates the Cr-substituted large pore MCM-48 materials can be easily obtained by using ammonia as the pH-adjusting agent. The initial Si/Cr ratio in the preparation system can be decreased to ten, which indicates that pH-adjusting method prefers to maintain the ordered mesostructure even at high Cr content. Moreover, it can also be observed that with the decrease in the Si/Cr ratio from 80 to 10, the (211) peak shifts to higher 2-θ angle, indicating that the d spacing decreases with the increasing Cr content. Table 1 summarizes the average unit cell parameter, a_0, of the as-synthesized and calcined samples with different Si/Cr ratios. In general, the incorporation of Cr with the covalent radius (1.18 Å) in tetrahedral geometry for Si (1.11 Å) is expected to slightly enlarge the a_0 value, which is confirmed by the increasing a_0 values of the as-synthesized samples with the increasing Cr incorporation amount as seen from Table 1. However, the a_0 values of the calcined samples gradually decrease with the increasing Cr content. The converse fact may be caused by the short double bond Cr=O in CrO_3 or Cr_2O_5, which indicates that most of the Cr species exist as Cr(VI) or Cr(V) in the calcined samples and as lower valent (Cr(III)) in the as-synthesized samples (Scheme 1).

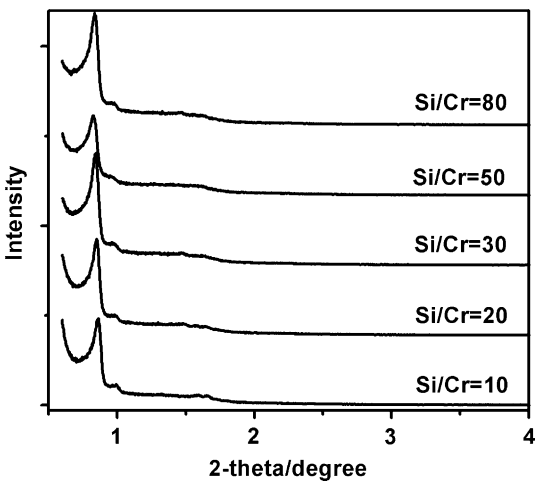

Fig. 1 XRD patterns of samples synthesized with different Si/Cr molar ratios at pH 6.0

Moreover, from Table 1, we can find that Cr species cannot be incorporated into the framework if the sample synthesized at Si/Cr = 80 does not experience the pH-adjustment treatment, and the pore size is only 6.3 nm, which is 3 nm less than the sample synthesized at the same Si/Cr ratio with the pH-adjustment treatment. In order to clarify whether the pore size enlargement is caused by the Cr incorporation or the pH-adjustment treatment, the pore size information of the sample synthesized with the pH adjustment in the absence of Cr is investigated. The result indicates that the Cr incorporation and pH adjustment are both advantageous to the enlargement of the pore size, but the pH-adjustment treatment is more effective, which increases the pore size from 6.3 to 8.8 nm. The enlargement of the pore by increasing the pH value to 6 in the absence of Cr may be due to the dissolution of the wall at higher pH value, since the thickness of the call calculated from the equation of (a_0/3.0919-Pd/2) decreases from 5.3 nm without the pH adjustment to 3.7 nm with the pH adjustment. Zhao et al. reported for the synthesis of SBA-15, when the pH values increase from 2 to 6, above the isoelectronic point of silica, no precipitation or formation of silica gel occurs [2]. In our synthesis system, the pH value is adjusted after the formation of mesoporous structure, which not only leads to the incorporation of Cr species into the framework, but also leads to the enlargement of the pore size, resulting in the formation of Cr-doped MCM-48-like mesoporous materials with pore size up to 10 nm.

Subsequently, the influence of pH to the formation of large pore MCM-48 material was investigated. Figure 2 shows XRD patterns of samples synthesized at Si/Cr = 50 and different pH. From the figure, we can find that with the increase of pH, the intensity of (211) peaks decrease, and the (220) peaks become more and more indistinct, indicating that higher pH is disadvantageous to the formation of ordered Cr-doped cubic mesostructure. It is known that the formation of mesoporous materials using P123 in acid system comply the route of $SH^+Cl^-I^+$ [2]. Although ammonia is added after the formation of cubic mesostructure, higher pH may still lead to the dissociation of the self-assembly system, thus destructing the formed mesostructure. Figure 3 shows the TEM images of samples prepared with Si/Cr = 50 at pH 5.0 (a–c) and pH 8.0 (d). From the figure, we can obviously find that the sample synthesized at pH 5.0 is more ordered than the sample synthesized at pH 8.0. However, the patterns along (110) (a and d) and (100) (b and c) directions confirm that both materials have cubic *Ia3d* symmetry.

Figure 4 shows the UV–Vis spectra of samples synthesized at various pH values with Si/Cr = 50. All the samples

Table 1 Structure parameters of calcined samples synthesized with different Si/Cr at pH 6.0

Si/Cr	ICP (wt%)	a_0^1 (nm)	a_0^2 (nm)	Pd (nm)	Wt (nm)	S_{BET} (m^2/g)	V_P (cm^3/g)
10	4.5	26.9	25.1	10.0	3.2	500	1.33
20	3.2	26.5	25.4	10.7	2.9	511	1.36
30	1.5	26.3	25.5	9.5	3.5	550	1.37
50	1.3	26.1	25.8	9.7	3.5	555	1.48
80	0.6	26.0	25.9	9.5	3.6	551	1.39
80^3	0	–	26.0	6.3	5.3	620	1.01
$\propto^4$	0	–	25.2	8.8	3.7	622	1.46

a_0^1 and a_0^2 are XRD unit cell parameters of the as-synthesized and calcined samples, respectively, S_{BET} is the apparent BET specific surface area deduced from BET isotherm in the relative pressure range of 0.05–0.30; V_P is the total pore volume determined from the adsorption branch of N_2 sorption isotherm at $P/P_0 = 1$; *Pd* is the pore diameter calculated using the BJH method. 80^3 is referred as the sample synthesized at Si/Cr = 80 without pH-adjustment process. $\propto^4$ is referred as the sample synthesized in the absence of Cr with the pH-adjustment process

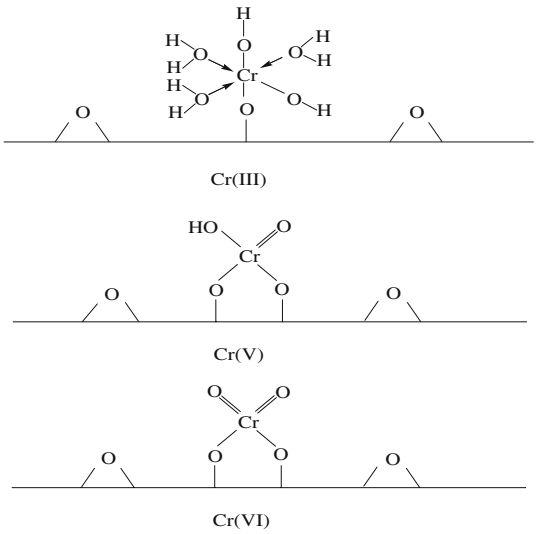

Scheme 1 Structure formula of Cr(III), Cr(V), and Cr(VI) oxides

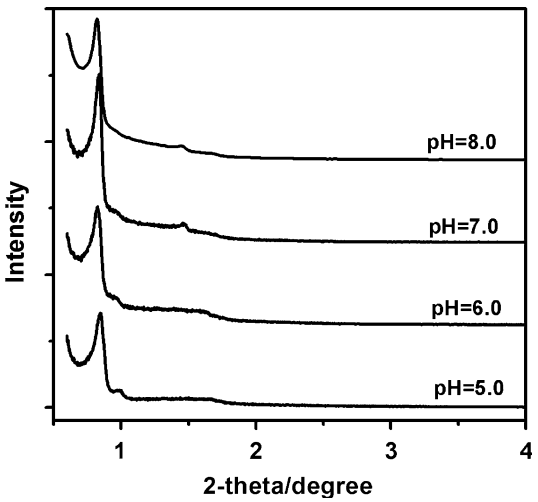

Fig. 2 XRD patterns of samples synthesized at Si/Cr = 50 and different pH

contain three bands around 260, 360, and 450 nm. The appearance of the former two intense bands is usually assigned as O→Cr (VI) charge transfer of chromate species [24–28]. The band shoulder around 450 nm is attributed to the absorption of Cr (VI) polychromate [29]. As shown in the figure, the sample synthesized at pH 6.0 has the strongest peak intensity, indicating the content of Cr (VI) chromate is the highest. With the increase or decrease of the pH in the second hydrothermal step, the intensity of adsorption decreases, indicating the content of Cr (VI) chromate decreases. The above results can be explained as follows: at low pH, Cr (III) ions are difficult to be incorporated into the framework because of the high solubility and loose interaction with silica walls. However, Cr (III) ions tend to form oxo species at higher pH, which are consequently grafted to the mesoporous walls through hydroxyl condensation and form Cr(VI) after calcination. However, too high pH leads to the rapid formation of precipitated hydrated Cr(III) oxide or chromic hydroxide ($Cr(OH)_3$) [29], which cannot be effectively incorporated into the mesoporous wall, either.

Since pH 6 is favorable to the formation of deposition and incorporation of Cr species into mesoporous material, we subsequently focused on studying the samples synthesized at pH 6. Figure 5 shows the nitrogen adsorption–desorption isotherms of the cubic large pore mesoporous materials prepared at pH = 6 with various Si/Cr ratios in the initial gel. As seen from Fig. 5a, all the samples show the sorption isotherms with typical type IV and H_1 hysteresis loop. A well-defined step, which occurs at a relatively high pressure of 0.7–0.9, corresponding to capillary condensation of N_2, indicates the uniformity of the pores, which is also proved by the pore size distribution curves (Fig. 5b). The structure parameters of calcined samples synthesized with different Si/Cr ratios are shown in Table 1. The pore sizes of these samples are larger than 10 nm. ICP-AES data show the weight percentages of the samples with Si/Cr molar ratios from 10 to 80 were 4.5%,

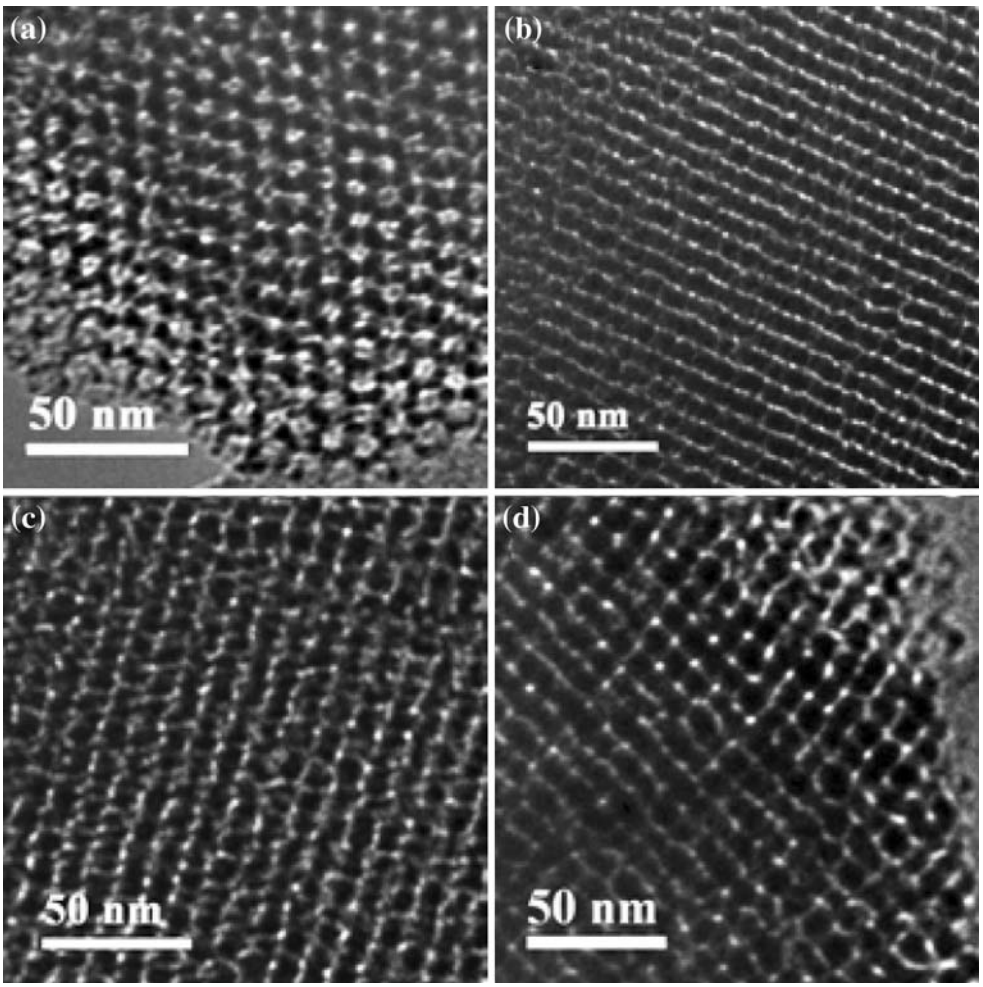

Fig. 3 TEM images of samples prepared at pH 5.0 (**a**–**c**) and pH 8.0 (**d**) with Si/Cr = 50

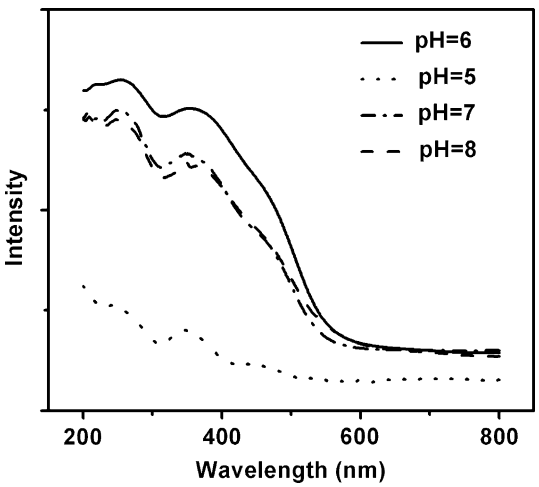

Fig. 4 UV–Vis spectra of samples synthesized at various pH with the Si/Cr ratio equal to 50

3.2%, 1.5%, 1.3%, and 0.6%, respectively, which indicate that the pH-adjusting method is an efficient way to incorporate large amount of chromium into the mesostructure.

Besides the pore structure, we also studied the Cr species in the above samples synthesized with different Si/Cr ratios by UV–vis spectra. As shown in Fig. 6, samples synthesized at Si/Cr = 80 and 50 have three adsorption bands around 260, 360, and 450 nm ascribing to Cr(VI) species. However, for the sample synthesized at Si/Cr = 30, a weak peak around 610 nm appears, which is attributed to the adsorption of Cr (III) species. The intensity of the band at 610 nm increases with increase in the Cr doping, indicating the rise of Cr (III) content [25]. Therefore, samples synthesized at higher Cr content contain both Cr (VI) chromate and Cr (III) species, but at lower Cr content, only Cr (VI) chromate can be detected.

The results from UV–Vis spectra are also confirmed by wide-angle XRD spectroscopy in Fig. 7. The broad peak at 2θ around 22° is assigned to the diffraction of silica skeleton. For the samples with low Cr loading (synthesized at Si/Cr = 50 and 80), no other peak appears, which indicates that no trivalent Cr_2O_3 cluster is formed. With the increase in the Cr content (Si/Cr $\leq$ 30), we can see weak diffraction signals at 2θ = 24.5°, 33.6°, 36.2°, and

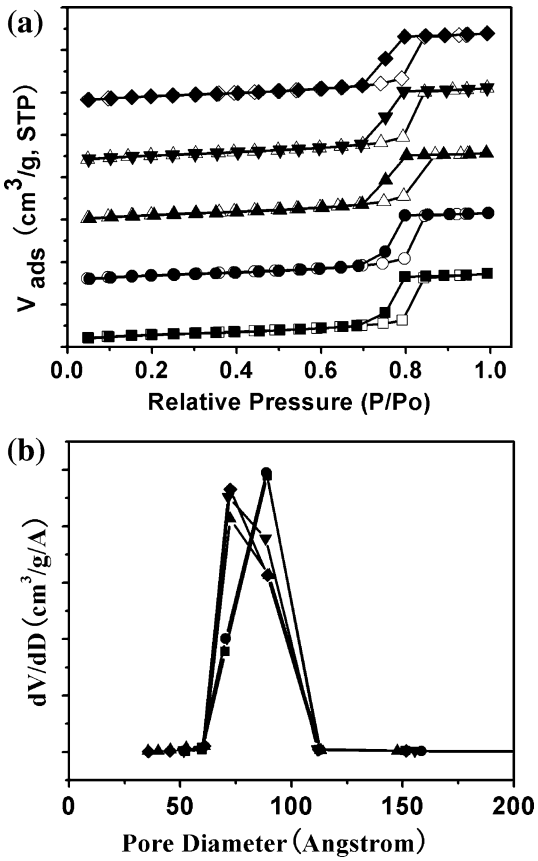

Fig. 5 Nitrogen adsorption–desorption isotherms (**a**) and BJH pore diameter distribution (**b**) of mesoporous materials synthesized at pH = 6. (*filled square*) Si/Cr = 10, (*filled circle*) Si/Cr = 20, (*filled triangle*) Si/Cr = 30, (*filled inverted triangle*) Si/Cr = 50, (*filled diamond*) Si/Cr = 80)

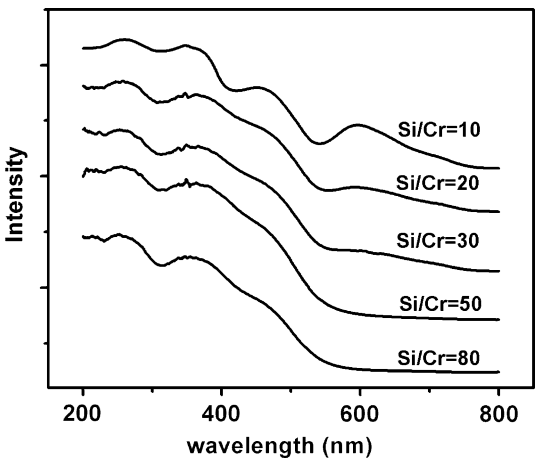

Fig. 6 UV-Vis spectra of calcined Cr incorporated mesoporous silica synthesized with different Si/Cr ratios at pH 6.0

54.8°, attributed to the hexagonal phase of Cr_2O_3 (JCPDS No.: 84-1616).

Moreover, the ESR spectra of samples (Fig. 8) synthesized with different Si/Cr ratios all show sharp signals at

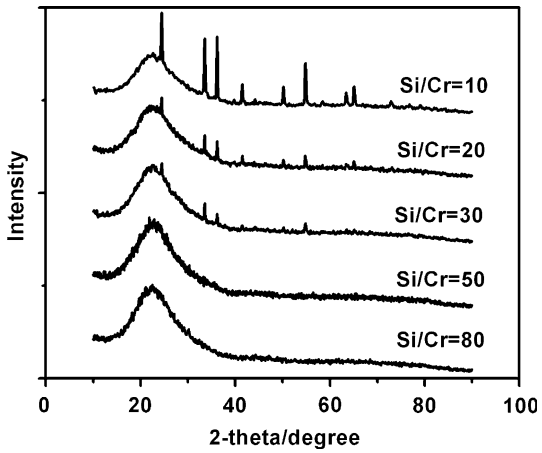

Fig. 7 Wide-angle XRD patterns of samples synthesized at pH 6.0 with different Si/Cr ratios

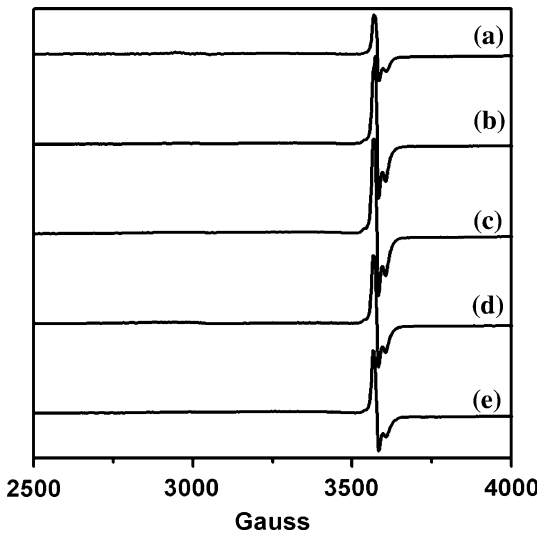

Fig. 8 ESR spectra of samples synthesized at pH = 6 with different Si/Cr molar ratios: (a) Si/Cr = 80; (b) Si/Cr = 50; (c) Si/Cr = 30; (d) Si/Cr = 20; (e) Si/Cr = 10

$g_\perp = 1.96$ and $g_\parallel = 1.97$, which are characteristic of Cr(V) in tetrahedral coordination [28] (see also Scheme 1). The results are in good agreement with literature, where chromium is present as both Cr(V) and Cr(VI) species [23, 28]. It was reported that three different Cr species can be detected with ESR: isolated Cr(V), clustered Cr(III) and dispersed Cr(III) [29]. From Fig. 6, we find that Cr_2O_3 is formed for the samples synthesized with Si/Cr $\leq$ 30. The lack of Cr(III) ESR signal in the samples with Si/Cr $\leq$ 30 indicates that there is only little amount of clustered Cr(III) or isolated Cr(III) in the higher Cr loading samples, leading to the negligible signal compared with Cr(V). The intensity of Cr(V) signal increases when the Si/Cr ratio decreases from 80 to 30, but cannot further increase when Si/Cr ratio

is less than 30, which indicates that most of the Cr(III) species transform to Cr(VI) after calcination.

Conclusions

A series of characterizing methods confirms that large-pore cubic *Ia3d* chromium-incorporated mesoporous silica was synthesized using pH-adjusting approach. This approach prefers the maintaining of highly ordered mesostructure even at high Cr content. However, too high pH is harmful to the formation of ordered mesostructure. For the sample synthesized at Si/Cr > 30, single site or low poly Cr(VI) and Cr(V) species dispersed in the framework. However, when the Si/Cr < 30, Cr(III) oxide species appear.

Acknowledgement This study has been supported by the Shanghai Natural Science Foundation (08ZR1406100), Morning Light Plan of Shanghai Education Development Foundation (2007CG040), Innovation Plan of Shanghai Municipality for Introduction of Foreign Technology (07XI-046), National High Technology Research and Development Program of China (2007AA05Z326), National Basic Research of China(973 Program 2004CB719500), National Nature Science Foundation of China (20773039), the Research Fund for the Doctoral Program of Higher Education(20070251006), and the Ministry of Science and Technology of China (2006AA06Z379, 2007AA 05Z303, 2006DFA52710).

References

1. Kresge CT, Leonowicz ME, Roth WJ, Vartuli JC, Beck JS (1992) Nature 359:710
2. Zhao DY, Feng JP, Huo QS, Melosh N, Fredrickson GH, Chmelka BF, Stucky GD (1998) Science 279:548
3. Liu XY, Tian BZ, Yu CZ, Gao F, Xie SH, Tu B, Che RC, Peng LM, Zhao DY (2002) Angew Chem Int Ed 41:3876
4. Flodström K, Alfredsson V, Källrot N (2003) J Am Chem Soc 125:4402
5. Kim TW, Kleitz F, Paul B, Ryoo R (2005) J Am Chem Soc 127:7601
6. Chen D, Li Z, Yu C, Shi Y, Zhang Z, Tu B, Zhao DY (2005) Chem Mater 17:3228
7. Chan YT, Lin HP, Mou CY, Liu ST (2002) Chem Commun 2878
8. Yue Y, Gideon A, Bonardet JL, Melosh N, D'Espinose JB, Fraissard J (1999) Chem Commun 1967
9. Han Y, Xiao FS, Wu S, Sun Y, Meng X, Li D, Lin S, Deng F, Ai X (2001) J Phy Chem B 105:7963
10. Newalkar BL, Olanrewaju J, Komarneni S (2001) Chem Mater 13:552
11. Zhang W, Lu Q, Han B, Li M, Xiu J, Ying P, Li C (2002) Chem Mater 14:3413
12. Wu S, Han Y, Zou YC, Song JW, Zhao L, Di Y, Liu SZ, Xiao FS (2004) Chem Mater 16:486
13. Luan Z, Bae JY, Kevan L (2000) Chem Mater 12:3202
14. Wh Y, Chen YJ, Min L, Fang H, Yan ZY, Wang HL, Wang JQ (2006) J Mol Catal A Chemical 246:162
15. Shao YF, Wang LZ, Zhang JL, Anpo M (2008) Micropor Mesopor Mater 109:271
16. Hamdy MS, Mul G, Wei W, Anand R, Hanefeld U, Jansen JC, Moulijn JA (2005) Catal Today 110:264
17. Wang YM, Wu ZY, Shi LY, Zhu JH (2005) Adv Mater 17:323
18. Wang YM, Wu ZY, Wang HJ, Zhu JH (2006) Adv Funct Mater 16:2374
19. Andersson M, Birkedal H, Franklin NR, Ostomel T, Boettcher S, Palmqvist Anders EC, Stucky GD (2005) Chem Mater 17:1409
20. Marianne MC, Bazin D, Appay MD, Beaunier P, Davidson A (2004) Chem Mater 16:1813
21. Wu ZY, Wang YM, Huang WW, Yang J, Wang HJ, Xu JH, Wei YL, Zhu JH (2007) Chem Mater 19:1613
22. Santamaria-Gonzalez J, Merida-Robles J, Alcantara-Rodriguez M, Maireles-Torres P, Rodriguez-Castellon E, Jimenez-Lopez A (2000) Catal Lett 64:209
23. Sakthivel A, Selvam P (2002) J Catal 211:134
24. Takehira K, Ohishi Y, Shishido T, Kawabata T, Takaki K, Zhang Q, Wang Y (2004) J Catal 224:404
25. Zhang L, Zhao Y, Dai H, He H, Au CT (2008) Catal Today 131:42
26. Selvaraj M, Kawi S (2007) Chem Mater 19:509
27. Wang Y, Ohishi Y, Shishido T, Zhang QH, Wang W, Guo Q, Wan HL, Takehira K (2003) J Catal 220:347
28. Zhu ZD, Chang ZX, Kevan L (1999) J Phys Chem B 103:2680
29. Weckhuysen BM, Wachs IE, Schoonheydt RA (1996) Chem Rev 96:3327